

# Entanglement and Bell nonlocality with bottom-quark pairs at hadron colliders

Yoav Afik,<sup>1,\*</sup> Yevgeny Kats,<sup>2,†</sup> Juan Ramón Muñoz de Nova,<sup>3,‡</sup> Abner Soffer,<sup>4,§</sup> and David Uzan<sup>2,¶</sup>

<sup>1</sup>*Enrico Fermi Institute, University of Chicago, Chicago, Illinois 60637, USA*

<sup>2</sup>*Department of Physics, Ben-Gurion University, Beer-Sheva 8410501, Israel*

<sup>3</sup>*Departamento de Física de Materiales, Universidad Complutense de Madrid, E-28040 Madrid, Spain*

<sup>4</sup>*School of Physics and Astronomy, Tel Aviv University, Tel Aviv 69978, Israel*

In the past years, it was shown that entanglement and Bell nonlocality, which are key concepts in Quantum Mechanics, can be probed in high-energy colliders, via processes of fundamental particle scattering. Recently, it has been shown that spin correlations can be measured in pairs of bottom quarks at the LHC. Given the low mass of the bottom quark compared to typical scattering processes at the LHC, many of the bottom-quark pairs are in the ultrarelativistic regime, where they can exhibit strong spin entanglement. We find that entanglement of bottom-quark pairs may be measurable even with Run 2 data, especially with the CMS  $B$  parking dataset, while observation of Bell nonlocality may become feasible at the high-luminosity phase of the LHC.

*Introduction.*—Entanglement is a fundamental property of Quantum Mechanics (QM) [1, 2]: if a pair of particles is entangled, the quantum state of the system cannot be described by specifying the state of each of the particles separately. A most remarkable manifestation of entanglement is the violation of Bell-type inequalities [3], which addresses the counter-intuitive absence of local realism. Both concepts are at the heart of QM, and have been probed in a variety of systems at different scales [4–12].

In recent years, it has been shown that quantum correlations are measurable in particle colliders, such as the LHC. Collider experiments offer a unique setup for these measurements, as they allow testing QM at the highest energies accessible to us. In particular, top-quark pair production at colliders has been studied extensively [13–23]. These proposals take advantage of the large mass of the top quark ( $m_t \approx 173$  GeV), resulting in an extremely short lifetime ( $\tau_t \approx 5 \times 10^{-25}$  s), significantly shorter than the typical time for hadronization ( $1/\Lambda_{\text{QCD}} \approx 3 \times 10^{-24}$  s) or spin decorrelation ( $m_t/\Lambda_{\text{QCD}}^2 \approx 2 \times 10^{-21}$  s). For this reason, the information of the top-quark pair spins is propagated directly to the decay products, allowing one to measure the polarizations and spin correlations of the top-quark pair system. Indeed, recent analyses by the ATLAS and CMS collaborations have observed quantum entanglement between a pair of top quarks for the first time [24, 25]. Other elementary particles such as neutrinos [26–28],  $\tau$  leptons [29–31], or massive gauge bosons [19, 32–37] also offer avenues for studying quantum correlations, as reviewed in Ref. [38].

Recently, it has been shown that measurement of spin correlations is possible not only in top-quark pairs, but also in pairs of lighter quarks [39]. In particular, bottom-quark pairs were found to be promising. Although the bottom quarks hadronize, their hadronization products can be used to measure their polarizations and spin correlations, albeit with some loss of precision. Since the bottom-quark mass is only  $m_b \approx 5$  GeV, a  $b\bar{b}$  pair is in the ultrarelativistic regime at a low invariant mass,  $M_{b\bar{b}}$ ,

compared to the  $t\bar{t}$  case. This makes the  $b\bar{b}$  system particularly attractive for study in this regime.

In this Letter we show that the LHC experiments ATLAS [40], CMS [41], and LHCb [42], with either standard or special trigger paths, are promising avenues for detecting entanglement and/or Bell nonlocality in  $b\bar{b}$  pairs. Some of the measurements can be pursued with data already collected, while others will become feasible at the high-luminosity phase of the LHC (HL-LHC).

*General Formalism.*—A  $b\bar{b}$  pair forms a bipartite system of two spin-1/2 particles. As such, it is described by the density matrix

$$\rho = \frac{I_4 + \sum_i (B_i^+ \sigma^i \otimes I_2 + B_i^- I_2 \otimes \sigma^i) + \sum_{i,j} C_{ij} \sigma^i \otimes \sigma^j}{4} \quad (1)$$

with  $I_n$  the  $n \times n$  identity matrix,  $B_i^\pm$  the components of the Bloch vectors  $\mathbf{B}^\pm$  that represent the quark/antiquark polarizations,  $C_{ij}$  the elements of the spin-correlation matrix  $\mathbf{C}$ , and  $\sigma^i$  the Pauli matrices.

At hadron colliders like the LHC, at leading order (LO) in quantum chromodynamics (QCD), bottom-quark pairs are produced from quark-antiquark ( $q\bar{q} \rightarrow b\bar{b}$ ) or gluon-gluon ( $gg \rightarrow b\bar{b}$ ) interactions. The kinematic state of a  $b\bar{b}$  pair in its center-of-mass (COM) frame is specified by the invariant mass  $M_{b\bar{b}}$  and the  $b$ -quark direction  $\hat{k}$ . For fixed  $(M_{b\bar{b}}, \hat{k})$ , the spin quantum state of the  $b\bar{b}$  pair is described by the density matrix  $\rho(M_{b\bar{b}}, \hat{k})$ , which is the weighted sum of the density matrices  $\rho^I(M_{b\bar{b}}, \hat{k})$  arising from the initial states  $I = q\bar{q}, gg$ ,

$$\rho(M_{b\bar{b}}, \hat{k}) = \sum_{I=q\bar{q}, gg} w_I(M_{b\bar{b}}) \rho^I(M_{b\bar{b}}, \hat{k}), \quad (2)$$

where the weights  $w_I$  are determined by the parton distribution functions (PDFs) that effectively describe the content and structure of the colliding hadrons. The polarizations and spin correlations of  $\rho(M_{b\bar{b}}, \hat{k})$  are described in terms of those of  $\rho^I(M_{b\bar{b}}, \hat{k})$  by equivalent expressions.

The orthonormal basis customarily used to evaluate  $B_i^\pm$  and  $C_{ij}$  is the helicity basis (e.g., Ref. [43]), defined

in the  $b\bar{b}$  COM frame in terms of the vectors  $\{\hat{k}, \hat{n}, \hat{r}\}$ . Here  $\hat{r} = (\hat{p} - \cos\Theta \hat{k})/\sin\Theta$  and  $\hat{n} = \hat{r} \times \hat{k}$ , where  $\hat{p}$  is the proton-beam axis, and  $\cos\Theta = \hat{k} \cdot \hat{p}$ . At LO in QCD, the  $b\bar{b}$  quantum state is unpolarized ( $B_i^\pm = 0$ ) and the non-vanishing spin-correlation matrix elements are  $C_{kk}, C_{nn}, C_{rr}, C_{rk} = C_{kr}$ . The analytical expressions for  $C_{ij}^I$  are solely functions of  $(M_{b\bar{b}}, \cos\Theta)$ , and given in Refs. [43–45].

The polarization and spin correlations for  $b\bar{b}$  pairs can be measured using events in which the  $b$  quarks hadronize into baryons. The lightest, most commonly produced  $b$ -baryon is the  $\Lambda_b$ , which in the simple quark model contains a spin-singlet, isospin-singlet combination of the light quarks  $u$  and  $d$  in addition to the  $b$  quark, which carries the baryon spin. Since  $m_b \gg \Lambda_{\text{QCD}}$ ,  $\Lambda_b$  baryons are expected to carry a large fraction of the original  $b$ -quark polarization [46–49]. The baryon polarization can be measured from the kinematic distribution of its decay products. This has been done, although with large statistical uncertainties, in  $Z \rightarrow b\bar{b}$  decays at LEP, using semileptonic decays of the  $\Lambda_b$  [50–52].

Spin-correlation measurements can be performed with both the  $\Lambda_b$  and  $\bar{\Lambda}_b$  decaying semileptonically via  $\Lambda_b \rightarrow X_c \ell^- \bar{\nu}_\ell$ , where  $X_c$  denotes a charmed state containing a baryon, usually the  $\Lambda_c^+$ . The angular distribution of the neutrinos from the two semileptonic decays is approximately [39]

$$\frac{1}{\sigma} \frac{d\sigma}{dx_{ij}} = \frac{1}{2} (1 - c_{ij} x_{ij}) \ln \left( \frac{1}{|x_{ij}|} \right), \quad (3)$$

where  $x_{ij} = \cos\theta_i^+ \cos\theta_j^-$ , the angles  $\theta_i^+$  and  $\theta_j^-$ , respectively, describe the momentum directions of the antineutrino (from the  $\Lambda_b$ ) and the neutrino (from the  $\bar{\Lambda}_b$ ) with respect to the basis axes  $i$  and  $j$  in the  $b\bar{b}$  COM frame, and

$$c_{ij} = \alpha^2 r_i r_j C_{ij}, \quad (4)$$

where  $\alpha \simeq 1$  is the spin analyzing power of the (anti)neutrino in the semileptonic  $\Lambda_b$  decay. The factors  $r_i$  and  $r_j$  are the longitudinal ( $r_L$ , for the  $\hat{k}$  axis) or transverse ( $r_T$ , for the  $\hat{n}$  and  $\hat{r}$  axes) polarization retention factors [48, 49]. They describe the fraction of the original quark's longitudinal or transverse polarization that is retained in the baryon and are rough approximations of the spin-dependent fragmentation functions (e.g., Refs. [53, 54]). Their values are expected to be roughly in the ranges  $0.4 \lesssim r_L \lesssim 0.8$ ,  $0.5 \lesssim r_T \lesssim 0.8$  [49] (see [55] for additional details), where the dominant polarization loss arises from  $\Lambda_b$  baryon production in  $\Sigma_b^{(*)}$  decays [48, 49]. An approximate combination of the LEP measurements [50–52] gives  $r_L = 0.47 \pm 0.14$ . It is also possible to measure  $r_L$  with competitive level of precision with the data already available in ATLAS and CMS, using the highly polarized  $b$  quarks from  $pp \rightarrow t\bar{t}$  events [49].

In addition, both  $r_L$  and  $r_T$  can be measured in  $pp \rightarrow b\bar{b}$  events [39]. This can be done independently of the entanglement measurement using a dedicated control region of phase space where significant entanglement is not expected while some of the elements  $C_{ij}$  are sizable.

Measuring  $C_{ij}$  requires reconstructing the momenta of the two  $b$ -quarks, the  $\Lambda_b$  baryons, and the neutrinos. This can be approximately done as outlined in Refs. [49, 56–60]. The approximations involved will need to be accounted for in interpreting the data and will lead to a reduction in sensitivity, the evaluation of which is beyond the scope of the current work.

*Entanglement and Bell Nonlocality.*—A quantitative measurement of entanglement is provided by the concurrence  $\mathcal{C}$  [61], which satisfies  $0 \leq \mathcal{C} \leq 1$ , where  $\mathcal{C} > 0$  is a sufficient and necessary condition for entanglement and  $\mathcal{C} = 1$  corresponds to a maximally entangled state. At LO QCD, the concurrence is given by  $\mathcal{C} = \max(\Delta, 0)$  [16], with

$$\Delta \equiv \frac{-C_{nn} + |C_{kk} + C_{rr}| - 1}{2}. \quad (5)$$

In general,  $\Delta > 0$  is always a sufficient condition for entanglement and can then be used as an entanglement marker.

Highly entangled states can violate Bell inequalities. For spin-1/2 particles, a useful form of Bell inequality is the Clauser-Horne-Shimony-Holt (CHSH) inequality [62], which involves projective spin measurements on each particle along alternate axes. A quantum state can violate CHSH inequality *iff*  $\mu_1 + \mu_2 > 1$ , with  $0 \leq \mu_2 \leq \mu_1 \leq 1$  the largest eigenvalues of  $\mathbf{C}^T \mathbf{C}$  [63]. In practice, a sufficient condition for CHSH violation is  $\mathcal{V} > 0$ , with

$$\mathcal{V} \equiv C_{kk}^2 + C_{rr}^2 - 1 \leq \mu_1 + \mu_2 - 1. \quad (6)$$

This observable is expected to accurately capture the Bell nonlocality of the  $b\bar{b}$  quantum state in the ultrarelativistic regime, where  $C_{kr} \simeq 0$  and  $C_{kk}^2, C_{rr}^2 > C_{nn}^2$ .

Figure 1 shows the concurrence of the  $b\bar{b}$  spin quantum state at the LHC, computed from Eq. (2), as a function of the invariant mass  $M_{b\bar{b}}$  and production angle  $\Theta$ ; here and in the following we use the NNPDF3.0 LO PDFs [64]. Entanglement (Bell nonlocality) takes place in the regions outside the solid white (dashed black) lines. Due to the dominance of the  $gg$  production channel, we can understand the entanglement structure in similar terms to that of  $t\bar{t}$  production [13, 16]. Close to threshold,  $M_{b\bar{b}} \simeq 2m_b$ , the  $b\bar{b}$  system is in a spin singlet, maximally entangled. However, in contrast to the  $t\bar{t}$  case, the threshold region is small relative to the range of  $M_{b\bar{b}}$  achievable at the LHC. In the ultrarelativistic regime,  $M_{b\bar{b}} \gg 2m_b$ , the  $b\bar{b}$  are in a maximally entangled spin-triplet state for transverse production ( $\cos\Theta \simeq 0$ ).

*Feasibility Study.*—We study the feasibility of measuring  $\Delta$  and  $\mathcal{V}$  at the LHC with Run 2 data and the fu-

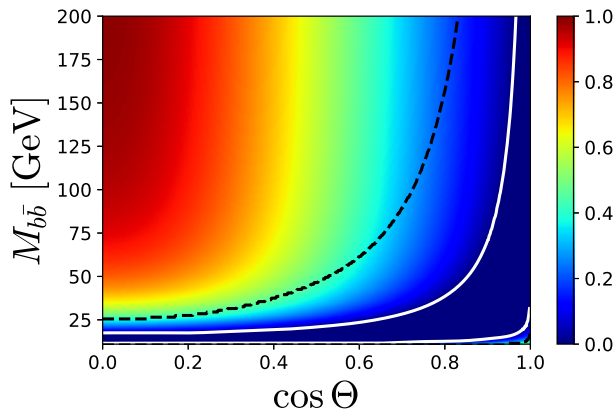


FIG. 1. Concurrence  $\mathcal{C}$  of the  $b\bar{b}$  quantum state  $\rho(M_{b\bar{b}}, \hat{k})$  at the LHC for  $pp$  collisions at a COM energy of  $\sqrt{s} = 13$  TeV, as a function of the invariant mass  $M_{b\bar{b}}$  and the production angle  $\Theta$  of the bottom quark in the  $b\bar{b}$  COM frame. The solid white (dashed black) line represents the critical boundary for entanglement (Bell nonlocality).

ture HL-LHC data [65, 66], assuming that similar triggers will be employed there. We consider the datasets of ATLAS/CMS (using the ATLAS parameters for our estimates) and LHCb, as well as the Run 2 CMS  $B$  parking dataset [67–70]. We use the estimated signal and background event counts from Ref. [39] for ATLAS, and perform additional simulations here to estimate the event counts for LHCb and the CMS  $B$  parking dataset, as well as compute the spin correlations for all cases.

We generate  $pp \rightarrow b\bar{b}$  events at LO QCD using the MadGraph [71] Monte Carlo (MC) generator and pass them through Pythia 8.3 [72] for parton showering, hadronization and decays. We use the anti- $k_T$  algorithm [73, 74] with  $R = 0.4$  for jet clustering and consider only the two leading  $p_T$   $b$ -jets in each event, in the pseudorapidity range  $2 < \eta < 5$  for LHCb,  $|\eta| < 2.4$  for Run 2 ATLAS and CMS, and  $|\eta| < 2.5$  for HL-LHC ATLAS and CMS. To estimate the event counts and spin correlations of the signal alone, we require the selection cuts on muons described below to be satisfied by muons produced directly in  $b$ -hadron decays and not in charmed-hadron decays or other sources, using truth MC information. We then use the binned truth parton-level values of  $M_{b\bar{b}}$  and  $\cos\Theta$  in the selected events to analytically compute the  $b\bar{b}$  spin correlation components for each bin [43].

In the analyses proposed for ATLAS, we rely on event selection via the double-muon trigger, which requires a pair of muons with  $p_T > 15$  GeV and  $|\eta| < 2.4$  in Run 2 or  $p_T > 10$  GeV and  $|\eta| < 2.5$  at the HL-LHC [75, 76]. Backgrounds from processes with prompt or mildly displaced muons (originating from charm or  $\tau$  decays) are assumed to be eliminated by a  $b$  tagging requirement, which needs to be satisfied by at least one of the jets, with an 80% efficiency for  $b$  jets. Backgrounds from  $c$ -

hadron decays in  $b$  jets, where the muons are typically softer than those produced directly in  $b$ -hadron decays, are assumed to be eliminated by applying the requirement  $z \equiv p_T^\mu/p_T^{\text{jet}} > 0.2$  to at least one of the muons. An important remaining background is due to semileptonic decays of  $B$  mesons. Reference [49] proposed three possible approaches to dealing with this background. The first approach (“Inclusive Selection”) does not attempt to reduce it. This results in low sample purity, but keeps the signal efficiency high. The  $B$ -meson background can be reduced (with a corresponding cost in signal statistics) by requiring the jet to contain a reconstructed  $\Lambda_c^+$  baryon (via one of its fully reconstructible decay modes, such as  $\Lambda_c^+ \rightarrow pK^-\pi^+$ ) or a  $\Lambda$  baryon (reconstructed via its  $\Lambda \rightarrow p\pi^-$  decay). These are referred to as “Exclusive Selection” and “Semi-Inclusive Selection”, respectively [49]. Each of these requirements can be applied to either one or both sides of the event, leading to six possible analysis channels, all of which were analyzed in [39]. The statistical uncertainty [55] was found to be the lowest for the inclusive/exclusive channel (although the other channels turned out rather comparable). The sample purity obtained in this channel is  $\sim 4.9\%$ . A higher sample purity of  $\sim 44\%$  is possible in the exclusive/exclusive channel at the price of lowering the signal efficiency by a factor of  $\sim 22$  and increasing the statistical uncertainty for the spin correlation components by a factor of  $\sim 1.6$ . We base our estimates on the inclusive/exclusive channel, while noting that sensitivity can be improved by combining all six channels or by utilizing electrons in addition to muons, which we do not pursue here. We estimate the number of signal events that will be available for the analysis as

$$N = 2\sigma_{b\bar{b}} \mathcal{L} f^2(b \rightarrow \Lambda_b) \text{BR}^2(\Lambda_b \rightarrow X_c \mu^- \bar{\nu}_\mu) \times \text{BR}(\Lambda_c^+ \rightarrow \text{reco.}) \epsilon_{\text{reco.}} \epsilon_{b,2} \epsilon_{z,2}, \quad (7)$$

where  $\sigma_{b\bar{b}}$  is the cross section after the cuts on muons but with the branching and fragmentation fractions factored out. For the fragmentation fraction, we use  $f(b \rightarrow \Lambda_b) \approx 7\%$  [49], except for hadrons with  $p_T < 25$  GeV where we implement a  $p_T$ -dependent enhancement of the  $\Lambda_b$  fragmentation fraction [77, 78] based on the results of Ref. [77]. This enhancement is important primarily for the LHCb analysis described below. Moreover, we use  $\text{BR}(\Lambda_b \rightarrow X_c \mu^- \bar{\nu}_\mu) \approx 11\%$ , and  $\text{BR}(\Lambda_c^+ \rightarrow \text{reco.}) \approx 18\%$  [79] for the list of channels included in Ref. [39]. The factor  $\epsilon_{\text{reco.}} \approx 50\%$  is our rough estimate for the average  $\Lambda_c^+$  decay reconstruction efficiency,  $\epsilon_{b,2} \equiv 2\epsilon_b - \epsilon_b^2$  is the efficiency for any of the two jets to pass the  $b$  tagging condition, and  $\epsilon_{z,2} \equiv 2\epsilon_z - \epsilon_z^2$  is the efficiency for any of the two muons to pass the  $p_T^\mu/p_T^{\text{jet}}$  cut mentioned above.

The CMS  $B$  parking dataset of Run 2 [67–70] is based on a trigger requiring a displaced muon with  $|\eta| < 1.5$  and  $p_T$  above thresholds between 7 and 12 GeV. The information on the integrated luminosity for each  $p_T$  threshold

	$\sigma_{b\bar{b}}$ [pb]	$\mathcal{L}$ [fb $^{-1}$ ]	$N$	$C_{kk}$	$C_{rr}$	$C_{nn}$	$\Delta$	$\mathcal{V}$	$r_L$	$\sigma_{\Delta}^{\text{stat}}$	$\sigma_{\mathcal{V}}^{\text{stat}}$	$\frac{\Delta}{\sigma_{\Delta}^{\text{stat}}}$	$\frac{\mathcal{V}}{\sigma_{\mathcal{V}}^{\text{stat}}}$	$\frac{\Delta}{\sigma_{\Delta}^{\text{tot}}}$	$\frac{\mathcal{V}}{\sigma_{\mathcal{V}}^{\text{tot}}}$
<b>Run 2, <math>\sqrt{s} = 13</math> TeV</b>															
ATLAS	$1.0 \times 10^4$	140	$1.4 \times 10^4$	0.96	0.62	-0.61	0.60	0.31	0.75	0.19	0.48	3.1	0.6	2.6	0.6
									0.45	0.32	1.11	1.8	0.3	1.7	0.3
LHCb, $\Delta > 0.4$	$2.7 \times 10^6$	5.7	$4.2 \times 10^4$	0.62	0.76	-0.66	0.52	-0.04	0.75	0.11	0.25	4.6	-0.1	3.4	-0.1
									0.45	0.19	0.46	2.7	-0.1	2.4	-0.1
CMS $B$ parking	$2.8 \times 10^5$	41.6	$3.7 \times 10^5$	0.88	0.61	-0.58	0.53	0.14	0.75	0.038	0.089	> 10	1.6	4.7	1.5
									0.45	0.064	0.20	8.4	0.7	4.3	0.7
<b>HL-LHC, <math>\sqrt{s} = 14</math> TeV</b>															
ATLAS, $\mathcal{V} > 0.3$	$3.9 \times 10^4$	3000	$6.2 \times 10^5$	0.94	0.86	-0.85	0.82	0.63	0.75	0.03	0.08	> 10	7.5	4.9	4.2
									0.45	0.05	0.17	> 10	3.7	4.8	3.0
LHCb, $\mathcal{V} > 0.3$	$3.2 \times 10^6$	300	$3.3 \times 10^5$	0.83	0.88	-0.83	0.77	0.48	0.75	0.040	0.11	> 10	4.3	4.8	3.3
									0.45	0.067	0.21	> 10	2.2	4.6	2.0
CMS $B$ parking, $\mathcal{V} > 0.2$	$3.1 \times 10^5$	800	$3.2 \times 10^6$	0.84	0.85	-0.80	0.75	0.43	0.75	0.013	0.035	> 10	> 10	5.0	4.6
									0.45	0.022	0.068	> 10	6.3	4.9	3.9

TABLE I. The cross section  $\sigma_{b\bar{b}}$  (after the cuts on muons but with the branching and fragmentation fractions factored out), integrated luminosity  $\mathcal{L}$ , number of expected signal events  $N$  (after the full selection), expected values for the diagonal spin correlation matrix elements, the quantities  $\Delta$  and  $\mathcal{V}$ , as well as their statistical uncertainties and significances. In the last two columns, we also show their total significance for a scenario with 20% systematic uncertainty. We present the statistical uncertainties for two values of the polarization retention factors  $r_i$  from Eq. (4): we fix  $r_T = 0.7$  and take an optimistic case of  $r_L = 0.75$  in the first subrow and a pessimistic case of  $r_L = 0.45$  in the second subrow.

(out of the total  $41.6 \text{ fb}^{-1}$ ) is available in Refs. [68, 69]. Our proposed analysis requires the presence of an additional muon (in another jet) with an opposite charge,  $p_T > 5 \text{ GeV}$  and  $|\eta| < 2.4$ . The advantage of this dataset is the higher statistics thanks to the low  $p_T$  thresholds relative to the typical ones used in CMS and ATLAS. We calculate the number of expected signal events accounting for the fact a muon is already required on one side:

$$N = 2f^2(b \rightarrow \Lambda_b) \text{BR}(\Lambda_b \rightarrow X_c \mu^- \bar{\nu}_\mu) \mathcal{A} \times \text{BR}(\Lambda_c^+ \rightarrow \text{reco.}) \epsilon_{\text{reco}} N_0, \quad (8)$$

where  $N_0 \approx 10^{10}$  is the number of  $b\bar{b}$  events in the CMS  $B$  parking dataset [67–70] (with an average purity of  $\approx 80\%$  [68]),  $\mathcal{A} \approx 38\%$  is the acceptance of selecting the muon on the non-triggering side of the event (found by our simulation) and, as in the previous case, we consider the inclusive/exclusive selection. We will also present the expected reach for the HL-LHC, in case such a trigger will be implemented. As an example, we will assume  $\mathcal{L} = 800 \text{ fb}^{-1}$  for the integrated luminosity and rescale  $N_0$  also by the ratio of our simulated cross section times acceptance at  $\sqrt{s} = 14$  vs. 13 TeV.

We also consider LHCb, which has lower integrated luminosity than ATLAS or CMS, but also lower trigger thresholds and better reconstruction capabilities. Motivated by Refs. [80, 81], we consider a trigger requiring a muon with  $p_T > 1.8 \text{ GeV}$  and  $2 < \eta < 5$ , a two-, three- or four-track secondary vertex with a significant displacement from any primary vertex (consis-

tent with a  $b$ -hadron decay), and a charged particle with  $p_T > 1.6 \text{ GeV}$  inconsistent with originating from a primary vertex. We simulate only the muon  $p_T$  and  $\eta$  requirements, assuming that the rest of the conditions will be satisfied for  $b\bar{b}$  events with an  $\mathcal{O}(1)$  efficiency. Our proposed analysis requires the presence of a second muon (in another jet) with an opposite charge,  $p_T > 0.5 \text{ GeV}$  and  $2 < \eta < 5$ . The number of expected signal events is computed with Eq. (7). The enhancement of the  $\Lambda_b$  fragmentation fraction at low  $p_T$  is important here. For the LHCb sample without any further cuts, our simulation gives the mean value  $\langle f(b \rightarrow \Lambda_b) f(\bar{b} \rightarrow \bar{\Lambda}_b) \rangle \approx 0.036$ .

Our results are presented in Table I. In some of the cases, as indicated, we applied an additional cut, on the expected parton-level value of  $\Delta$  or  $\mathcal{V}$  for the event, to increase the  $\Delta$  or  $\mathcal{V}$  significance in the sample. In these cases, for LHCb we also required  $M_{b\bar{b}} > 20 \text{ GeV}$  at the parton level to focus on the ultrarelativistic entangled regime. We have explicitly checked that directly averaging the value of  $\mathcal{V}$  in phase space, which should increase the signal due to the convexity of Bell locality [16, 22], does not lead to a sensible improvement in the significance of the observation.

We find that the CMS  $B$  parking dataset is the most promising avenue for detecting entanglement in Run 2 data, with statistical significance of roughly  $10\sigma$ , with the exact number depending on the values of the polarization retention factors  $r_L$  and  $r_T$ . This leaves room for obtaining high significance even after accounting for the systematic uncertainties. LHCb may also be able



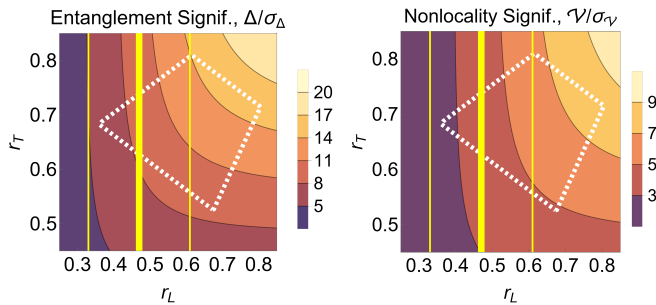


FIG. 2. The expected statistical significance of entanglement in Run 2 CMS  $B$  parking dataset (left) and Bell nonlocality in the ATLAS HL-LHC data with the  $\mathcal{V} > 0.3$  cut (right) as a function of the polarization retention factors  $r_L$  and  $r_T$ . The white dotted polygons approximately indicate the region of plausible values for  $r_L$  and  $r_T$  [48, 49, 55]. The vertical yellow lines show the central value of  $r_L$  (thick line) and its  $\pm 1\sigma$  uncertainties (thin lines) from an approximate combination of the LEP measurements [50–52].

to produce a meaningful measurement, especially if  $r_L$  and  $r_T$  happen to be high. At the HL-LHC all the experiments are promising for detecting entanglement with high significance, and show potential for detecting Bell nonlocality as well. In Fig. 2 we show how the statistical significance depends on  $r_L$  and  $r_T$  for the measurement of entanglement with the CMS  $B$  parking dataset of Run 2 and the measurement of Bell nonlocality with the ATLAS HL-LHC dataset.

*Conclusions and Discussion.*—We propose methods to measure entanglement and Bell nonlocality at the LHC with pairs of  $b\bar{b}$  quarks. This system is especially attractive given the large cross section for ultrarelativistic bottom quarks at the LHC. We find that the observation of entanglement is possible with high significance with the currently available CMS  $B$  parking data, while Bell nonlocality is still beyond our current reach but will be accessible using the full HL-LHC data. We find that entanglement observation is also possible in LHCb, further motivating the study of quantum correlations at this detector.

In future work, it will be useful to extend the predictions for  $b\bar{b}$  spin correlations beyond LO QCD. It will also be interesting to explore the possibility of measuring entanglement and Bell nonlocality in future colliders, such as the FCC-ee and the FCC-hh [82–84], with different production mechanisms. Furthermore, other QM concepts, such as discord and steering [18], can be also addressed in  $b\bar{b}$  pairs. In general, our work paves the way to study quantum correlations in hadronizing systems. Among others, this could have impact on the characterization of the quark-gluon plasma, whose vortical structure can lead to non-trivial spin properties [85]. The direct access to the ultrarelativistic regime provided by bottom quarks can be also of interest for the study of the relativistic behavior of the spin operator, a fundamental

question in QM which is still open [86–92].

YA is supported by the National Science Foundation under Grant No. PHY-2013010. YK and DU are supported in part by the Israel Science Foundation (Grant No. 1666/22) and the United States - Israel Binational Science Foundation (Grant No. 2018257). JRMdN is supported by European Union’s Horizon 2020 research and innovation programme (Marie Skłodowska-Curie Grant Agreement No. 847635), and by Spain’s Agencia Estatal de Investigación (Grant No. PID2022-139288NB-I00). AS is supported by the Israel Science Foundation (grant Nos. 203/23 and 3464/21), the United States-Israel Binational Science Fund (grant No. 2020044), and the Horizon 2020 Marie Skłodowska-Curie RISE project JENNIFER2 (grant No. 822070).

## SUPPLEMENTAL MATERIAL

### Polarization retention factors

As analyzed in [48] and developed further in [49], in the heavy-quark limit, the polarization retention factors in  $b \rightarrow \Lambda_b$  fragmentation can be expressed in terms of two nonperturbative QCD parameters,  $A$  and  $w_1$ , as

$$r_L \approx \frac{1 + A(0.23 + 0.38w_1)}{1 + A}, \quad (9)$$

$$r_T \approx \frac{1 + A(0.62 - 0.19w_1)}{1 + A}. \quad (10)$$

These quantities,  $r_L$  and  $r_T$ , are the fractions of the initial  $b$ -quark polarization (in the longitudinal and transverse directions, respectively, relative to the fragmentation axis, i.e., the  $b$  quark momentum direction) that are retained in the final  $\Lambda_b$  polarization. The above expressions describe the dominant polarization loss effect, due to the contribution to the  $\Lambda_b$  sample from  $\Sigma_b^{(*)} \rightarrow \Lambda_b \pi$  decays. The parameter

$$A = \frac{\text{prob}(\Sigma_b^{(*)})}{\text{prob}(\Lambda_b)} = 9 \frac{\text{prob}(T)}{\text{prob}(S)} \quad (11)$$

is the ratio of the  $\Sigma_b^{(*)}$ -decay and direct  $\Lambda_b$  production rates. It is related to the probability for the two light quarks in the baryon to form any of the nine spin-triplet, isospin-triplet diquark states  $T$  and the probability to form the spin-singlet, isospin-singlet diquark state  $S$ . The statistical hadronization model (for a brief overview, see [93]) predicts  $A \approx 2.6$  [49], but it is unclear how accurate this number is. The parameter

$$w_1 = \frac{\text{prob}(T_{\pm 1})}{\text{prob}(T)} \quad (12)$$

accounts for the possibility that the fragmentation axis breaks the rotational symmetry in the spin-triplet diquark production. It describes the probability for the

diquark to be produced with spin component  $+1$  or  $-1$  (but not  $0$ ) along the fragmentation axis. The isotropic case is obtained for  $w_1 = 2/3$ . The value of  $w_1$  can be determined from the angular distributions of the pions in the  $\Sigma_b^{(*)} \rightarrow \Lambda_b \pi$  decays [48, 49]. Measurements of both  $A$  and  $w_1$  can certainly be done at LHCb [94] and perhaps even at ATLAS and CMS. The white dotted polygons in Fig. 2 of the main text correspond to the range

$$1 \leq A \leq 5, \quad 0 \leq w_1 \leq 1, \quad (13)$$

where the chosen range for  $A$  reflects a large systematic uncertainty.

### Statistical uncertainty estimation

The expected statistical uncertainty in a measurement of the spin correlation matrix components  $C_{ij}$ , using a fit of the data to Eq. (3) from the main text and the relation in Eq. (4) therein, is approximately [39]

$$\sigma_{C_{ij}}^{\text{stat}} \simeq \frac{3}{r_i r_j \alpha^2 \sqrt{fN}}, \quad (14)$$

where  $N$  is the expected number of signal events after the full event selection,  $f$  is the sample purity  $N/(N + N_B)$ , with  $N_B$  being the number of background events, and we have approximated the angular distribution of the background to be similar to that for  $C_{ij} = 0$ .

---

\* yoavafik@gmail.com

† katsye@bgu.ac.il

‡ jrmnova@fis.ucm.es

§ asoffer@tau.ac.il

¶ daviduz@post.bgu.ac.il

- [1] A. Einstein, B. Podolsky, and N. Rosen, Can quantum mechanical description of physical reality be considered complete?, *Phys. Rev.* **47**, 777 (1935).
- [2] E. Schrodinger, Discussion of probability relations between separated systems, *Pro. Cambridge Phi. Soc.* **31**, 555 (1935).
- [3] J. S. Bell, On the Einstein-Podolsky-Rosen paradox, *Physics Physique Fizika* **1**, 195 (1964).
- [4] A. Aspect, P. Grangier, and G. Roger, Experimental Realization of Einstein-Podolsky-Rosen-Bohm Gedankenexperiment: A New Violation of Bell's Inequalities, *Phys. Rev. Lett.* **49**, 91 (1982).
- [5] E. Hagley, X. Maitre, G. Nogues, C. Wunderlich, M. Brune, J. M. Raimond, and S. Haroche, Generation of Einstein-Podolsky-Rosen Pairs of Atoms, *Phys. Rev. Lett.* **79**, 1 (1997).
- [6] M. Steffen, M. Ansmann, R. C. Bialczak, N. Katz, E. Lucero, R. McDermott, M. Neeley, E. M. Weig, A. N. Cleland, and J. M. Martinis, Measurement of the entanglement of two superconducting qubits via state tomography, *Science* **313**, 1423 (2006).
- [7] W. Pfaff, T. H. Taminiau, L. Robledo, H. Bernien, M. Markham, D. J. Twitchen, and R. Hanson, Demonstration of entanglement-by-measurement of solid-state qubits, *Nature Physics* **9**, 29 (2013).
- [8] A. Go *et al.* (Belle), Measurement of EPR-type flavour entanglement in  $\Upsilon(4S) \rightarrow B^0 \bar{B}^0$  decays, *Phys. Rev. Lett.* **99**, 131802 (2007), arXiv:quant-ph/0702267.
- [9] B. Julsgaard, A. Kozhekin, and E. S. Polzik, Experimental long-lived entanglement of two macroscopic objects, *Nature* **413**, 400 (2001).
- [10] K. Lee, M. Sprague, B. Sussman, J. Nunn, N. Langford, X.-M. Jin, T. Champion, P. Michelberger, K. Reim, D. England, D. Jaksch, and I. Walmsley, Entangling macroscopic diamonds at room temperature, *Science (New York, N.Y.)* **334**, 1253 (2011).
- [11] C. F. Ockeloen-Korppi, E. Damskagg, J.-M. Pirkkalainen, M. Asjad, A. A. Clerk, F. Massel, M. J. Woolley, and M. A. Sillanpää, Stabilized entanglement of massive mechanical oscillators, *Nature* **556**, 478 (2018).
- [12] S. Storz *et al.*, Loophole-free Bell inequality violation with superconducting circuits, *Nature* **617**, 265 (2023).
- [13] Y. Afik and J. R. Muñoz de Nova, Entanglement and quantum tomography with top quarks at the LHC, *Eur. Phys. J. Plus* **136**, 907 (2021), arXiv:2003.02280 [quant-ph].
- [14] M. Fabbrichesi, R. Floreanini, and G. Panizzo, Testing Bell Inequalities at the LHC with Top-Quark Pairs, *Phys. Rev. Lett.* **127**, 161801 (2021), arXiv:2102.11883 [hep-ph].
- [15] C. Severi, C. D. E. Boschi, F. Maltoni, and M. Sioli, Quantum tops at the LHC: from entanglement to Bell inequalities, *Eur. Phys. J. C* **82**, 285 (2022), arXiv:2110.10112 [hep-ph].
- [16] Y. Afik and J. R. Muñoz de Nova, Quantum information with top quarks in QCD, *Quantum* **6**, 820 (2022), arXiv:2203.05582 [quant-ph].
- [17] J. A. Aguilar-Saavedra and J. A. Casas, Improved tests of entanglement and Bell inequalities with LHC tops, *Eur. Phys. J. C* **82**, 666 (2022), arXiv:2205.00542 [hep-ph].
- [18] Y. Afik and J. R. Muñoz de Nova, Quantum Discord and Steering in Top Quarks at the LHC, *Phys. Rev. Lett.* **130**, 221801 (2023), arXiv:2209.03969 [quant-ph].
- [19] R. Ashby-Pickering, A. J. Barr, and A. Wierzychucka, Quantum state tomography, entanglement detection and Bell violation prospects in weak decays of massive particles, *JHEP* **05** (2023), 020, arXiv:2209.13990 [quant-ph].
- [20] Z. Dong, D. Gonçalves, K. Kong, and A. Navarro, When the Machine Chimes the Bell: Entanglement and Bell Inequalities with Boosted  $t\bar{t}$ , (2023), arXiv:2305.07075 [hep-ph].
- [21] J. A. Aguilar-Saavedra, Postdecay quantum entanglement in top pair production, *Phys. Rev. D* **108**, 076025 (2023), arXiv:2307.06991 [hep-ph].
- [22] K. Cheng, T. Han, and M. Low, Optimizing Fictitious States for Bell Inequality Violation in Bipartite Qubit Systems, (2023), arXiv:2311.09166 [hep-ph].
- [23] J. A. Aguilar-Saavedra, A closer look at post-decay  $t\bar{t}$  entanglement, *Phys. Rev. D* **109**, 096027 (2024), arXiv:2401.10988 [hep-ph].
- [24] G. Aad *et al.* (ATLAS), Observation of quantum entanglement in top-quark pairs using the ATLAS detector, (2023), arXiv:2311.07288 [hep-ex].

- [25] *Probing entanglement in top quark production with the CMS detector*, Tech. Rep. CMS-PAS-TOP-23-001 (CERN, Geneva, 2024).
- [26] J. A. Formaggio, D. I. Kaiser, M. M. Murskyj, and T. E. Weiss, Violation of the Leggett-Garg Inequality in Neutrino Oscillations, *Phys. Rev. Lett.* **117**, 050402 (2016), [arXiv:1602.00041 \[quant-ph\]](#).
- [27] F. Ming, X.-K. Song, J. Ling, L. Ye, and D. Wang, Quantification of quantumness in neutrino oscillations, *Eur. Phys. J. C* **80**, 275 (2020).
- [28] M. Blasone, S. De Siena, and C. Matrella, Wave packet approach to quantum correlations in neutrino oscillations, *Eur. Phys. J. C* **81**, 660 (2021), [arXiv:2104.03166 \[quant-ph\]](#).
- [29] M. Fabbrichesi, R. Floreanini, and E. Gabrielli, Constraining new physics in entangled two-qubit systems: top-quark, tau-lepton and photon pairs, *Eur. Phys. J. C* **83**, 162 (2023), [arXiv:2208.11723 \[hep-ph\]](#).
- [30] M. M. Altakach, P. Lamba, F. Maltoni, K. Mawatari, and K. Sakurai, Quantum information and CP measurement in  $H \rightarrow \tau^+\tau^-$  at future lepton colliders, *Phys. Rev. D* **107**, 093002 (2023), [arXiv:2211.10513 \[hep-ph\]](#).
- [31] K. Ehatäht, M. Fabbrichesi, L. Marzola, and C. Veelken, Probing entanglement and testing Bell inequality violation with  $e^+e^- \rightarrow \tau^+\tau^-$  at Belle II, *Phys. Rev. D* **109**, 032005 (2024), [arXiv:2311.17555 \[hep-ph\]](#).
- [32] A. J. Barr, Testing Bell inequalities in Higgs boson decays, *Phys. Lett. B* **825**, 136866 (2022), [arXiv:2106.01377 \[hep-ph\]](#).
- [33] A. J. Barr, P. Caban, and J. Rembieliński, Bell-type inequalities for systems of relativistic vector bosons, *Quantum* **7**, 1070 (2023), [arXiv:2204.11063 \[quant-ph\]](#).
- [34] J. A. Aguilar-Saavedra, A. Bernal, J. A. Casas, and J. M. Moreno, Testing entanglement and Bell inequalities in  $H \rightarrow ZZ$ , *Phys. Rev. D* **107**, 016012 (2023), [arXiv:2209.13441 \[hep-ph\]](#).
- [35] J. A. Aguilar-Saavedra, Laboratory-frame tests of quantum entanglement in  $H \rightarrow WW$ , *Phys. Rev. D* **107**, 076016 (2023), [arXiv:2209.14033 \[hep-ph\]](#).
- [36] A. Bernal, P. Caban, and J. Rembieliński, Entanglement and Bell inequalities violation in  $H \rightarrow ZZ$  with anomalous coupling, *Eur. Phys. J. C* **83**, 1050 (2023), [arXiv:2307.13496 \[hep-ph\]](#).
- [37] R. A. Morales, Exploring Bell inequalities and quantum entanglement in vector boson scattering, *Eur. Phys. J. Plus* **138**, 1157 (2023), [arXiv:2306.17247 \[hep-ph\]](#).
- [38] A. J. Barr, M. Fabbrichesi, R. Floreanini, E. Gabrielli, and L. Marzola, Quantum entanglement and Bell inequality violation at colliders, (2024), [arXiv:2402.07972 \[hep-ph\]](#).
- [39] Y. Kats and D. Uzan, Prospects for measuring quark polarization and spin correlations in  $b\bar{b}$  and  $c\bar{c}$  samples at the LHC, *JHEP* **03** (2024), 063, [arXiv:2311.08226 \[hep-ph\]](#).
- [40] G. Aad *et al.* (ATLAS), The ATLAS Experiment at the CERN Large Hadron Collider, *JINST* **3** (2008), S08003.
- [41] S. Chatrchyan *et al.* (CMS), The CMS Experiment at the CERN LHC, *JINST* **3** (2008), S08004.
- [42] A. A. Alves, Jr. *et al.* (LHCb), The LHCb Detector at the LHC, *JINST* **3** (2008), S08005.
- [43] M. Baumgart and B. Tweedie, A New Twist on Top Quark Spin Correlations, *JHEP* **03** (2013), 117, [arXiv:1212.4888 \[hep-ph\]](#).
- [44] W. Bernreuther and A. Brandenburg, Tracing CP violation in the production of top quark pairs by multiple TeV proton proton collisions, *Phys. Rev. D* **49**, 4481 (1994), [arXiv:hep-ph/9312210](#).
- [45] W. Bernreuther, M. Flesch, and P. Haberl, Signatures of Higgs bosons in the top quark decay channel at hadron colliders, *Phys. Rev. D* **58**, 114031 (1998), [arXiv:hep-ph/9709284](#).
- [46] T. Mannel and G. A. Schuler, Semileptonic decays of bottom baryons at LEP, *Phys. Lett. B* **279**, 194 (1992).
- [47] F. E. Close, J. G. Körner, R. J. N. Phillips, and D. J. Summers, Report of the b-fragmentation working group. Section 5: b polarization at LEP, *J. Phys. G* **18**, 1703 (1992).
- [48] A. F. Falk and M. E. Peskin, Production, decay, and polarization of excited heavy hadrons, *Phys. Rev. D* **49**, 3320 (1994), [arXiv:hep-ph/9308241](#).
- [49] M. Galanti, A. Giammanco, Y. Grossman, Y. Kats, E. Stamou, and J. Zupan, Heavy baryons as polarimeters at colliders, *JHEP* **11** (2015), 067, [arXiv:1505.02771 \[hep-ph\]](#).
- [50] D. Buskulic *et al.* (ALEPH), Measurement of the  $\Lambda_b$  polarization in Z decays, *Phys. Lett. B* **365**, 437 (1996).
- [51] G. Abbiendi *et al.* (OPAL), Measurement of the average polarization of b baryons in hadronic  $Z^0$  decays, *Phys. Lett. B* **444**, 539 (1998), [arXiv:hep-ex/9808006](#).
- [52] P. Abreu *et al.* (DELPHI),  $\Lambda_b$  polarization in  $Z^0$  decays at LEP, *Phys. Lett. B* **474**, 205 (2000).
- [53] A. Metz and A. Vossen, Parton Fragmentation Functions, *Prog. Part. Nucl. Phys.* **91**, 136 (2016), [arXiv:1607.02521 \[hep-ex\]](#).
- [54] K. Chen, G. R. Goldstein, R. L. Jaffe, and X.-D. Ji, Probing quark fragmentation functions for spin-1/2 baryon production in unpolarized  $e^+e^-$  annihilation, *Nucl. Phys. B* **445**, 380 (1995), [arXiv:hep-ph/9410337](#).
- [55] See Supplemental Material, which includes Refs. [93, 94].
- [56] S. Dambach, U. Langenegger, and A. Starodumov, Neutrino reconstruction with topological information, *Nucl. Instrum. Meth. A* **569**, 824 (2006), [arXiv:hep-ph/0607294](#).
- [57] R. Aaij *et al.* (LHCb), Determination of the quark coupling strength  $|V_{ub}|$  using baryonic decays, *Nature Phys.* **11**, 743 (2015), [arXiv:1504.01568 \[hep-ex\]](#).
- [58] R. Aaij *et al.* (LHCb), First Observation of the Decay  $B_s^0 \rightarrow K^- \mu^+ \nu_\mu$  and a Measurement of  $|V_{ub}|/|V_{cb}|$ , *Phys. Rev. Lett.* **126**, 081804 (2021), [arXiv:2012.05143 \[hep-ex\]](#).
- [59] G. Ciezarek, A. Lupato, M. Rotondo, and M. Vesterinen, Reconstruction of semileptonically decaying beauty hadrons produced in high energy  $pp$  collisions, *JHEP* **02** (2017), 021, [arXiv:1611.08522 \[hep-ex\]](#).
- [60] S. Dambach, *CMS pixel module readout optimization and study of the  $B^0$  lifetime in the semileptonic decay mode*, Ph.D. thesis, Heidelberg U. (2009).
- [61] W. K. Wootters, Entanglement of formation of an arbitrary state of two qubits, *Phys. Rev. Lett.* **80**, 2245 (1998).
- [62] J. F. Clauser, M. A. Horne, A. Shimony, and R. A. Holt, Proposed experiment to test local hidden-variable theories, *Phys. Rev. Lett.* **23**, 880 (1969).
- [63] R. Horodecki, P. Horodecki, and M. Horodecki, Violating Bell inequality by mixed spin-1/2 states: necessary and sufficient condition, *Phys. Lett. A* **200**, 340 (1995).

- [64] R. D. Ball *et al.* (NNPDF), Parton distributions for the LHC Run II, *JHEP* **04** (2015), 040, [arXiv:1410.8849 \[hep-ph\]](#).
- [65] I. Béjar Alonso *et al.* (Eds.), *High-Luminosity Large Hadron Collider (HL-LHC): Technical design report*, Tech. Rep. CERN-2020-010 (CERN, Geneva, 2020).
- [66] *Framework TDR for the LHCb Upgrade II: Opportunities in flavour physics, and beyond, in the HL-LHC era*, Tech. Rep. CERN-LHCC-2021-012, LHCb-TDR-023 (CERN, Geneva, 2021).
- [67] R. Bainbridge (CMS), Recording and reconstructing 10 billion unbiased b hadron decays in CMS, *EPJ Web Conf.* **245**, 01025 (2020).
- [68] A. Hayrapetyan *et al.* (CMS), Enriching the physics program of the CMS experiment via data scouting and data parking, (2024), [arXiv:2403.16134 \[hep-ex\]](#).
- [69] A. Hayrapetyan *et al.* (CMS), Test of lepton flavor universality in  $B^\pm \rightarrow K^\pm \mu^+ \mu^-$  and  $B^\pm \rightarrow K^\pm e^+ e^-$  decays in proton-proton collisions at  $\sqrt{s} = 13$  TeV, (2024), [arXiv:2401.07090 \[hep-ex\]](#).
- [70] A. Hayrapetyan *et al.* (CMS), Search for long-lived heavy neutrinos in the decays of B mesons produced in proton-proton collisions at  $\sqrt{s} = 13$  TeV, (2024), [arXiv:2403.04584 \[hep-ex\]](#).
- [71] J. Alwall, R. Frederix, S. Frixione, V. Hirschi, F. Maltoni, O. Mattelaer, H. S. Shao, T. Stelzer, P. Torrielli, and M. Zaro, The automated computation of tree-level and next-to-leading order differential cross sections, and their matching to parton shower simulations, *JHEP* **07** (2014), 079, [arXiv:1405.0301 \[hep-ph\]](#).
- [72] T. Sjöstrand, S. Ask, J. R. Christiansen, R. Corke, N. Desai, P. Ilten, S. Mrenna, S. Prestel, C. O. Rasmussen, and P. Z. Skands, An introduction to PYTHIA 8.2, *Comput. Phys. Commun.* **191**, 159 (2015), [arXiv:1410.3012 \[hep-ph\]](#).
- [73] M. Cacciari, G. P. Salam, and G. Soyez, The anti- $k_t$  jet clustering algorithm, *JHEP* **04** (2008), 063, [arXiv:0802.1189 \[hep-ph\]](#).
- [74] M. Cacciari, G. P. Salam, and G. Soyez, FastJet User Manual, *Eur. Phys. J. C* **72**, 1896 (2012), [arXiv:1111.6097 \[hep-ph\]](#).
- [75] G. Aad *et al.* (ATLAS), Performance of the ATLAS muon triggers in Run 2, *JINST* **15** (2020), P09015, [arXiv:2004.13447 \[physics.ins-det\]](#).
- [76] *Expected performance of the ATLAS detector at the High-Luminosity LHC*, Tech. Rep. ATL-PHYS-PUB-2019-005 (CERN, Geneva, 2019).
- [77] R. Aaij *et al.* (LHCb), Measurement of b hadron fractions in 13 TeV pp collisions, *Phys. Rev. D* **100**, 031102 (2019), [arXiv:1902.06794 \[hep-ex\]](#).
- [78] R. Aaij *et al.* (LHCb), Enhanced Production of  $\Lambda_b^0$  Baryons in High-Multiplicity pp Collisions at  $\sqrt{s} = 13$  TeV, *Phys. Rev. Lett.* **132**, 081901 (2024), [arXiv:2310.12278 \[hep-ex\]](#).
- [79] R. L. Workman *et al.* (Particle Data Group), Review of Particle Physics, *PTEP* **2022**, 083C01 (2022).
- [80] R. Aaij *et al.* (LHCb), Test of lepton universality with  $B^0 \rightarrow K^{*0} \ell^+ \ell^-$  decays, *JHEP* **08** (2017), 055, [arXiv:1705.05802 \[hep-ex\]](#).
- [81] R. Aaij *et al.* (LHCb), Amplitude analysis of the  $\Lambda_c^+ \rightarrow p K^- \pi^+$  decay and  $\Lambda_c^+$  baryon polarization measurement in semileptonic beauty hadron decays, *Phys. Rev. D* **108**, 012023 (2023), [arXiv:2208.03262 \[hep-ex\]](#).
- [82] A. Abada *et al.* (FCC), FCC-ee: The Lepton Collider: Future Circular Collider Conceptual Design Report Volume 2, *Eur. Phys. J. ST* **228**, 261 (2019).
- [83] A. Abada *et al.* (FCC), FCC-hh: The Hadron Collider: Future Circular Collider Conceptual Design Report Volume 3, *Eur. Phys. J. ST* **228**, 755 (2019).
- [84] M. Benedikt, A. Blondel, P. Janot, M. Mangano, and F. Zimmermann, Future Circular Colliders succeeding the LHC, *Nature Phys.* **16**, 402 (2020).
- [85] L. Adamczyk *et al.* (STAR), Global  $\Lambda$  hyperon polarization in nuclear collisions: evidence for the most vortical fluid, *Nature* **548**, 62 (2017), [arXiv:1701.06657 \[nucl-ex\]](#).
- [86] M. Czachor, Einstein-Podolsky-Rosen-Bohm experiment with relativistic massive particles, *Phys. Rev. A* **55**, 72 (1997), [arXiv:quant-ph/9609022](#).
- [87] R. M. Gingrich and C. Adami, Quantum Entanglement of Moving Bodies, *Phys. Rev. Lett.* **89**, 270402 (2002), [arXiv:quant-ph/0205179](#).
- [88] A. Peres and D. R. Terno, Quantum information and relativity theory, *Rev. Mod. Phys.* **76**, 93 (2004), [arXiv:quant-ph/0212023](#).
- [89] N. Friis, A. R. Lee, K. Truong, C. Sabin, E. Solano, G. Johansson, and I. Fuentes, Relativistic Quantum Teleportation with superconducting circuits, *Phys. Rev. Lett.* **110**, 113602 (2013), [arXiv:1211.5563 \[quant-ph\]](#).
- [90] J. Rembieliński and P. Caban, Relativistic chiral qubits, their time evolution, and correlations, *Phys. Rev. A* **99**, 022320 (2019).
- [91] F. Giacomini, E. Castro-Ruiz, and Č. Brukner, Relativistic Quantum Reference Frames: The Operational Meaning of Spin, *Phys. Rev. Lett.* **123**, 090404 (2019), [arXiv:1811.08228 \[quant-ph\]](#).
- [92] P. Kurashvili and L. Chotorlishvili, Quantum discord and entropic measures of two relativistic fermions, *J. Phys. A* **55**, 495303 (2022), [arXiv:2207.12963 \[hep-th\]](#).
- [93] A. Andronic, F. Beutler, P. Braun-Munzinger, K. Redlich, and J. Stachel, Statistical hadronization of heavy flavor quarks in elementary collisions: Successes and failures, *Phys. Lett. B* **678**, 350 (2009), [arXiv:0904.1368 \[hep-ph\]](#).
- [94] R. Aaij *et al.* (LHCb), Observation of Two Resonances in the  $\Lambda_b^0 \pi^\pm$  Systems and Precise Measurement of  $\Sigma_b^\pm$  and  $\Sigma_b^{*\pm}$  properties, *Phys. Rev. Lett.* **122**, 012001 (2019), [arXiv:1809.07752 \[hep-ex\]](#).